PIFA DESIGN FOR DUAL BAND OPERATION IN MOBILE

ABSTRACT

Planar Inverted F Antenna (PIFA) has long been considered as a prominent candidate for integration into mobile devices due to its compact size, low profile, and versatility in design. Adopted from [1] which design a PIFA operating at 2.6 GHz and 3.6 GHz, this letter presents a model that function at the resonance frequency of 0.9 GHz and 1.8 GHz (LTE 3 and LTE 8 respectively). Beginning with a primitive design of monoband antenna using equation (1) from [2], the author of this report optimizes the length and width of the PIFA for the lower frequency (0.9 GHz). Afterwards, meandered slot inherited from [1] will be utilized to create the second resonance frequency at 1.8 GHz. Additionally, this letter uses FR04 substrate (relative permittivity = 4.4) in the design with the aim at decreasing the dimensions of antenna. The length and width of the substrate are 140 mm and 70 mm respectively, resembling the size of a real smartphone. The metal plate is situated at the bottom of the substrate which has a width of 7 mm. The shorting pin or plate will short the planar antenna to the ground, whereas the feeding pin will provide energy for the antenna as coaxial cable. Even though the form of the slot and the parasitic element are inspired by a predesigned antenna, this report's final design take different structure, form, material, and operating frequencies. The results show that the design is capable of operating at two desired frequencies. Even though the radiating efficiency at the lower frequency is not up to par, the return losses at both frequencies suffice with good radiating efficiency at the higher frequency. Additionally, potential ideas and design are also presented for improving the radiating efficiency at the lower frequency.

Duc Anh Trinh

EEL4461 – Antenna Theory

Introduction

In the rapidly evolving trend of mobile communication, the demand for enhanced connectivity and efficiency has surged, driven by the fast-growing reliance on smartphones, tablets, and other portable devices that can be seen by everyday usage. To meet this demand, the design and optimization of antenna design in mobile devices play a vital role, especially in achieving multi-band functionality for expanded frequency coverage and improved performance.

This report focuses on the development and implementation of Planar Inverted-F Antenna (PIFA) designs tailored for dual-band operation in mobile devices. PIFA antenna have been given significant attention in recent years due to their compact form factor, low profile, and suitability for integration into electronics devices. By leveraging these characteristics of PIFA, the author aims to show the design process and results associated with dual-band PIFA operation, such as frequency isolation, impedance matching, and radiation efficiency. The primitive simulation shows that with approximately the same dimensions, the design of shorting plate in PIFA yields better match in resonance frequency than that of shorting pin.

The proliferation of wireless communication standards, including 5G, Wi-Fi 6, and emerging IoT protocols, necessitates versatile antenna solutions capable of operating across multiple frequency bands without compromising performance. Dual-band PIFA designs offer a promising avenue to achieve this goal, enabling diverse connectivity across various networks while mitigating interference and signal degradation.

In this letter, the author delves into the theoretical foundations of PIFA design, redesigning the PIFA of another paper and parameters influencing its performance. Subsequently, the author explores various strategies for realizing dual-band functionality within the constraints of this letter’s desired frequency.

Furthermore, the author presents simulation results and performance evaluations of prototype dual-band PIFA implementations, assessing key metrics such as return loss, radiation patterns, and bandwidth characteristics. Through comprehensive analysis and optimization, the author demonstrates the ability of integrating dual-band PIFA antennas into mobile devices, thereby enhancing their connectivity in the desired frequency.

Overall, this report contributes to advancing the pre-designed PIFA idea into new mobile communication antenna design in different frequency, offering insights and methodologies for the design of compact dual-band PIFA solutions.

By bridging the gap between theoretical understanding and practical implementation, the author aims to facilitate his knowledge obtained during the lecture meeting into real-world applications and simulations.

Antenna Design

Design Considerations

The antenna design is inspired by paper [1], in which a dual-band PIFA is proposed to resonate at 2.6 GHz and 3.5 GHz. The design procedures in this paper are described as follows. Firstly, the dimensions of the PIFA are chosen so as to operate in the lower frequency of the dual frequency. After the optimization process, they proceed to add meandered slot with a "snake' form to bring the fifth resonating frequency down to the desired frequency. Finally, they add a capacitive parasitic element of quarter-wavelength to improve the bandwidth of that second resonating frequency.

The length and width of the substrate are 150 mm and 70 mm respectively, resembling the size of a real smartphone. The metal plate is situated at the bottom of the substrate which has a width of 7 mm. The shorting pin or plate will short the planar antenna to the ground, whereas the feeding pin will provide energy for the antenna as coaxial cable.

To begin with, the author considers the design of PIFA to resonate at f = 0.9 Hz with shorting plate along the width of planar antenna and coaxial feeding pin. Using equation (1) with f = 0.9 GHz, $\varepsilon_r = 4.4$, the PIFA's dimensions after optimizing are L = 38.5 mm, W = L/1.5 mm, W_shortplate = L/3, H = 0.7 mm; the Antenna and its dimensions are shown in **Figure 1**, and its return loss are shown in **Figure 2**. As expected, there are two resonating frequencies observed, one at around 0.9 GHz and the other at around 2.7 GHz (third order resonating frequencies). However, the return loss for the PIFA at 0.9 GHz showed poor performance since the criteria for a good operating point is considered to be below -10 dB. Meanwhile, the third order resonating frequencies at 2.7 shows a much better return loss at -15 dB. Therefore, the author decided to move to the second PIFA design, which places the shorting plate at the long side of the antenna and drives the PIFA with the same purpose of resonating frequency is at 0.9 GHz. After recalculating the PIFA's dimensions with the dimension L using equation (2) from rectangular patch antenna theory and optimizing, the dimensions are L = 95.4 mm, W = 35.8 mm, H = 0.7 mm, and the shorting plate's width is equal to the long side of the radiating patch as shown in **Figure 3**. Equation (2) is used to calculate L because L will be cancelled if w_s is

equal to L according to equation (1), which that is in this case. After this step, I proceed to adding the slot to the antenna.

Slot Design

There are many slotting techniques and forms provided in the literature to obtain multiband operation, with the dual band being the simplest. Originally, U-slot and L-slot are extensively studied and implemented due to its simplicity and effectiveness. However, other shapes including the mix and matching between U-shape and L-shape have gained more interest in the PIFA field. For example, two groups of slots are added to the existing current path in [2]. The first group includes a U-shaped piece and an L-shaped one. The second group comprises a straight slot with open ends placed between the two parts of the first group. Another innovative slot form is introduced in [3]. To achieve improved impedance matching across all frequencies and adequately cover the desired bands, an array of orthogonal slots is implemented on the patch to make a crossed shape.

As previously mentioned, the form of the slot is inspired by the design in [1], in which they reason that the slot should not interfere with the main radiating frequency. To do so, the current distribution at the frequency is plot, and the slot is placed in a way such that it omits the regions where the current is large. The current distribution is shown in **Figure 4**, which led to the opening slot starting at the long side of the antenna and extending to the short side of the antenna because those are the regions with the least current distribution. **Figure 5** shows the structure of this slot. The width of the slot is taken from [1], which is 0.7 mm, and the total length of the slot is around quarter wavelength of the lower frequency, also taken from the same paper. Importantly, all these slots share the same width. In the CAD program, the slot is created simply by designing the structure of each branch of the slot and subtracting the slot from the antenna. As a result, the return loss is obtained and shown in **Figure 6**.

Experimental Optimization

After obtaining acceptable return loss parameters, the antenna's radiation efficiency is studied by computing the antenna parameters in HFSS design with equation (3). The accepted power and radiation power of the slotted PIFA at the two resonant frequency is shown in **Figure 7**, and the radiation efficiencies are 54% and 56% at 0.9 GHz and 1.8 GHz respectively. Even though the reflection power (expressed through return loss graph) is low enough, expressed through high accepted power, to be deemed adequate, normally below -6 dB for PIFA antenna, the obtained radiation efficiency is low in this letter's design. Another common challenge in PIFA antenna is the narrow bandwidth, which

generates less useful coverage frequencies. Building upon the traditional U-Slot method for enhancing PIFA (Planar Inverted-F Antenna) performance, [4] presents a parallel Dual-slot PIFA design that outperforms the U-Slot both in terms of performance and ease of manufacturing, operating at single frequency. Additionally, [1] realizes the bandwidth challenges and introduce a parasitic element of quarter wavelength next to the main radiating patch. Nevertheless, the antenna return loss parameter will suffer.

First, a quarter-wavelength parasitic element is placed next to the antenna to observe the effect of it on the bandwidth and antenna's return loss parameters. The parasitic element requires further optimization since it shifts the return loss to the left. The resulting return loss is shown in **Figure 8**, which shows that the parasitic improves the performance of the higher resonating frequency in both bandwidth and return loss but deteriorates the both the return loss and radiation efficiency of the lower resonating frequency. **Figure 9** shows the accepted and radiated power at two resonant frequencies, which demonstrates 62% efficiency at 1.8 GHz but only 45% at 0.9 GHz.

Some designs have been applied with the intention of increasing the radiation efficiency at the lower resonating for this report but have not been successful. However, I will include those efforts in this letter for the merit of completeness. For example, bandwidth can be improved by adding slots to the metal plate ground plane [5] as shown in **Figure 10**, but that is not achieved in this report's simulation. After observing the current distribution in the main radiating plate, I also tried adding a similar slot mirrored through the middle axis as shown in **Figure 11**, but the return loss yields poor results.

Comparison to the Original Design

Table 1. Comparison of two Design

Parameters	[1]'s Design	This report's Design
Resonating Frequency	2.6 GHz and 3.5 GHz	0.9 GHz and 1.8 GHz
Substrate	Air	FR4 ($\varepsilon_r = 4.4$)
Feed	Coaxial Cable	
Short	Metal Plate on short side	Metal Plate on long side
Antenna Dimension (mm)	L = 21, W = 11, H = 7.7	L = 93.4, W = 32.8, H = 7
Slot Total Length (mm)	27.8	46.3
Parasitic Element Dimension (mm)	7*1.3	28*13
Ground Dimension (mm)	140*70	
Return Loss at lower frequency	-17dB	-13dB
Return Loss at upper frequency	-33dB	-16dB

All of the conductor of the design used in this report is copper with the height of 0.3 mm. The coaxial cable dielectric's material is Teflon.

The 3D radiation pattern, 2D polar plot in azimuth and elevation plane, and input impedance are shown from **Figure 12** onward. The radiation at the lower resonant frequency presented in **Figure 12** is a typical pattern of a patch antenna, with the radiation direction in the theta = 0 direction with minimum back radiation, which is a crucial advantage for mobile devices since it minimizes the bad effects on human's head. **Figure 13** shows the radiation pattern at the second resonant frequency with 3.44 dB Gain. The radiation can be described as the shape of two radiation at the lower frequency in parallel. Importantly, it still behaves with minimal back radiating characteristics. Compared to the existing literatures, the radiation pattern at the higher resonant frequency is similar. The corresponding 2D plot of the radiation pattern for azimuth and elevation plane is from **Figure 14** to **16**, which allows to observe the directivity as well as the non-back-radiating characteristics of PIFA. **Figure 17** illustrates the Smith Chart of the input impedance of the report's design. The objective of this chart is to support the design process in which the resonant frequencies are tried to be brough down the zero-line. **Figure 18** presents more straightforward input impedances information, in which the top and bottom figure show the real and imaginary impedance respectively. The real part is almost 50 Ohms, whereas the imaginary impedance is near to 0. This design, therefore, is not best optimized. However, optimization is not a linear process, so to efficiently bring the impedance to its matching point and keep the resonant frequency at desired point at the same requires more study.

Conclusion

In conclusion, this report focusses on the development and implementation of Planar Inverted-F Antenna (PIFA) designs tailored for dual-band operation in mobile devices. With the advantage of PIFA such as compactness and less back-radiating, the concentration on dual-band PIFA designs is driven by the need to support multiple wireless communication standards while maintaining small form factors suitable for integration into portable devices.

Drawing inspiration from existing literature, particularly [1], this report presents a systematic approach to designing dual-band PIFA antennas. Through theoretical foundations and experimental optimization, various design considerations such as substrate material, feeding mechanism, shorting configuration, and slot design are explored and analyzed. Simulation results demonstrate the effectiveness of the proposed designs in achieving dual-band functionality at 0.9 GHz and 1.8 GHz, with considerations for return loss, radiation efficiency, and bandwidth characteristics.

Despite challenges such as narrow bandwidth and low radiation efficiency, efforts to optimize the design through the addition of parasitic elements and slot modifications are discussed. Comparison with the original design from [1] highlights the differences in resonating frequencies, substrate material, feeding mechanism, and antenna dimensions.

Overall, this report contributes to advancing the author's understanding and implementation of dual-band PIFA antennas for mobile communication applications. By bridging theoretical concepts with practical simulations and optimizations, it provides insights and methodologies for designing compact and efficient antenna solutions capable of supporting dual-band communication standards in modern mobile devices.

Equation and Figures

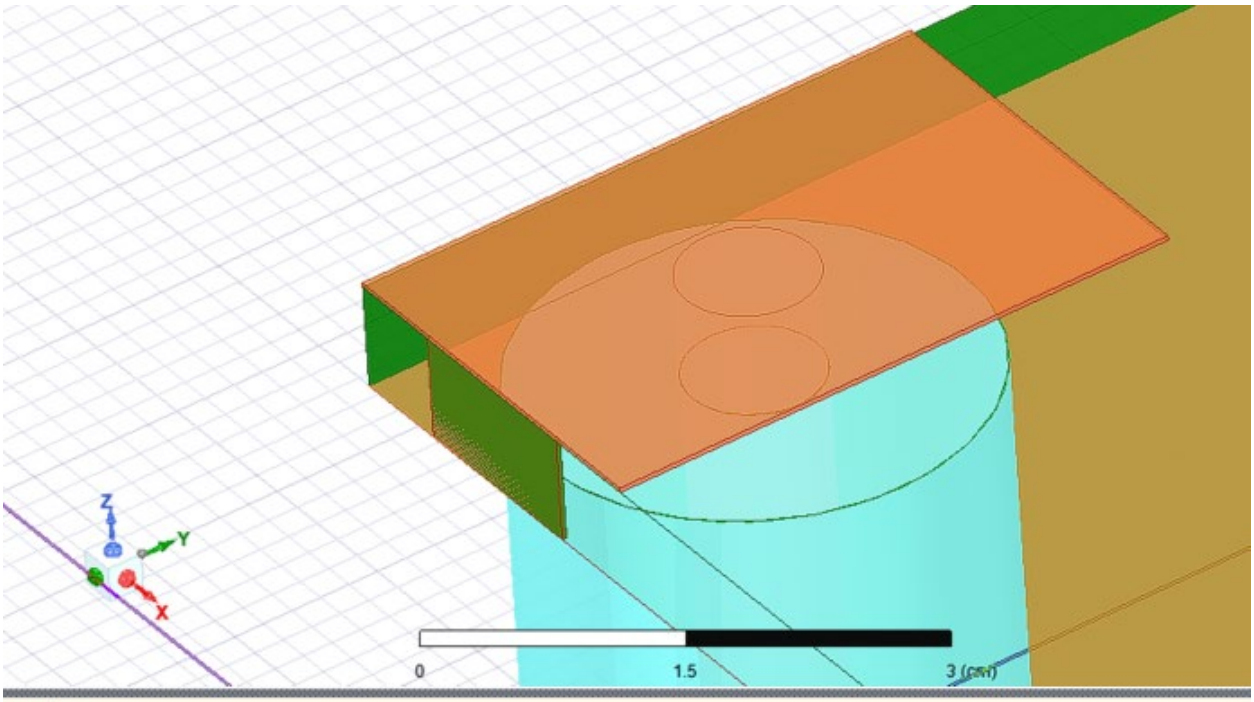

roperties

Name	Value	Unit	Evaluated V...	Typ
–Antenna Dimensions				
patchX	patchY/1.5		25.666667mm	Design
patchY	38.5	mm	38.5mm	Design
–Shorting Plate Dimensions				
plateW	patchX/2		12.833333mm	Design

Figure 1. PIFA resonating at 0.9 Hz with shorting plate in the short side.

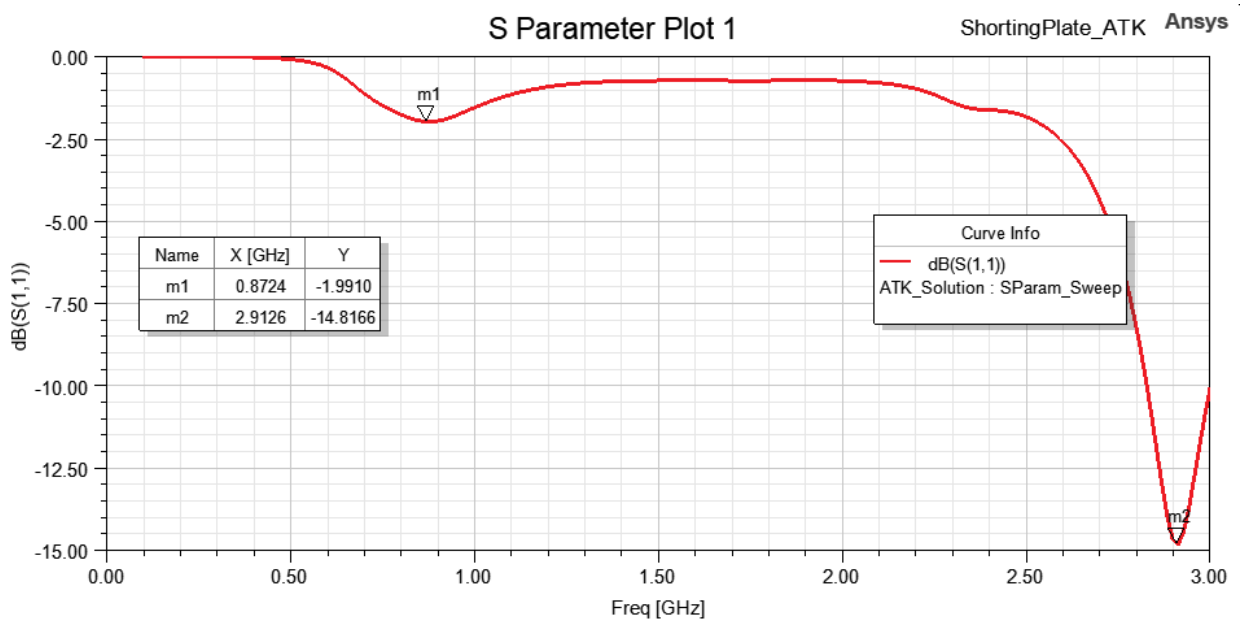

Figure 2. S Parameter for the antenna shown in **Figure 1**

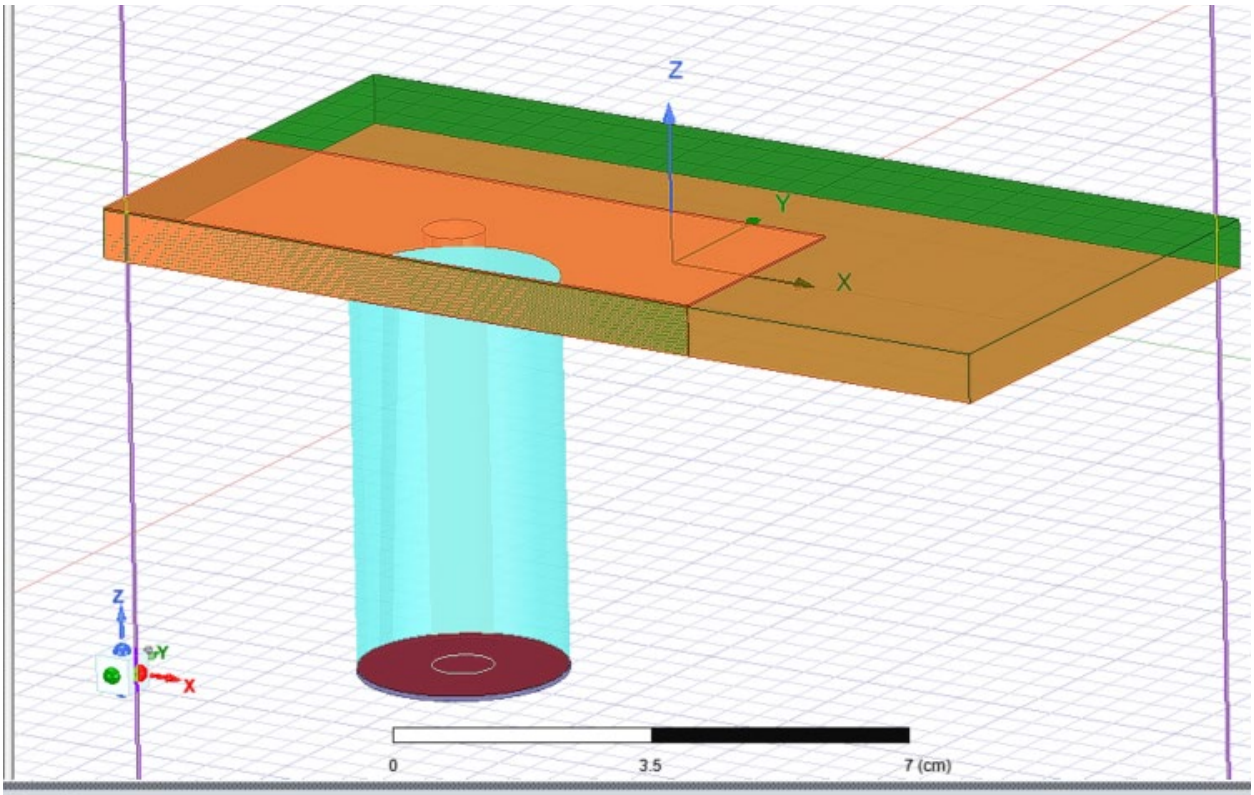

Properties

Name	Value	Unit	Evaluated V...	Type
–Antenna Dimensions				
patchX	94.4	mm	94.4mm	Design
patchY	35.8	mm	35.8mm	Design
–Shorting Plate Dimensions				
plateW	patchX		94.4mm	Design
–Substrate Dimensions				
subH	0.7	cm	0.7cm	Design
subX	14	cm	14cm	Design

Figure 3. PIFA resonating at 0.9 GHz with the shorting plate on the long side.

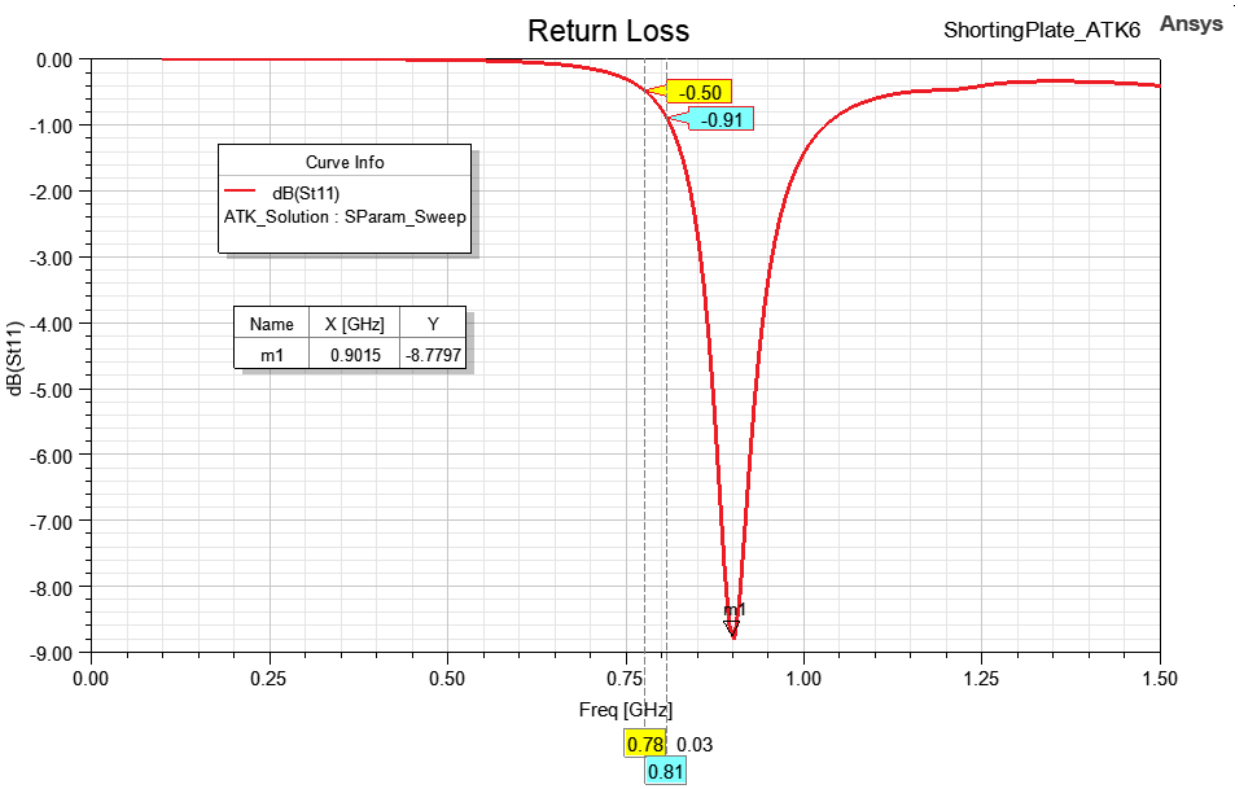

Figure 4. S11 Parameter of the antenna in **Figure 3**

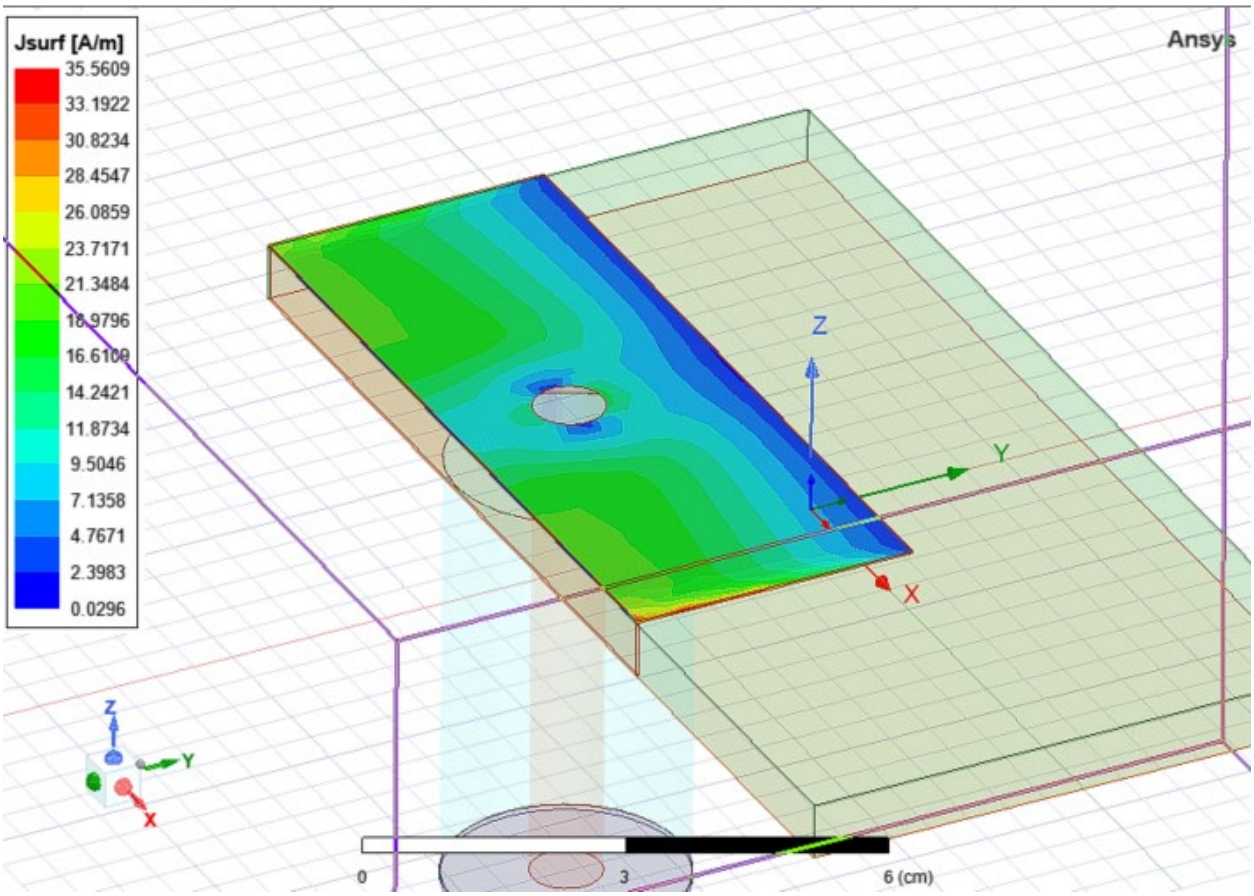

Figure 4. Current Distribution at 0.9 GHz

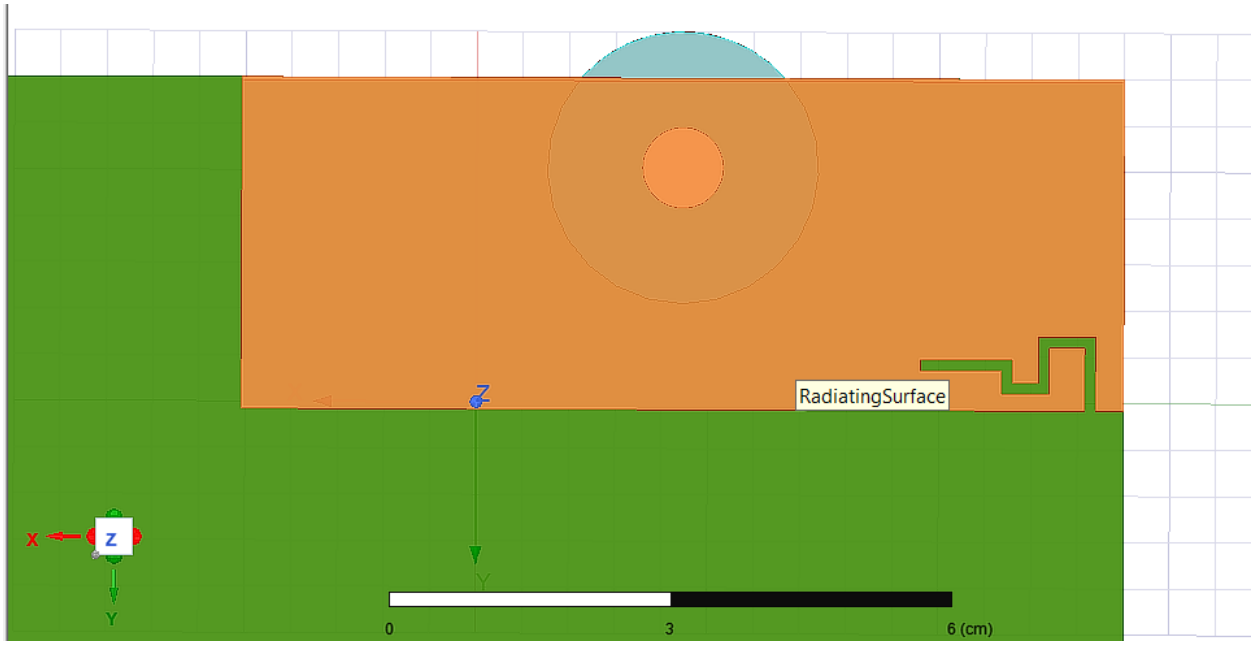

Figure 5. Slot Structure in PIFA

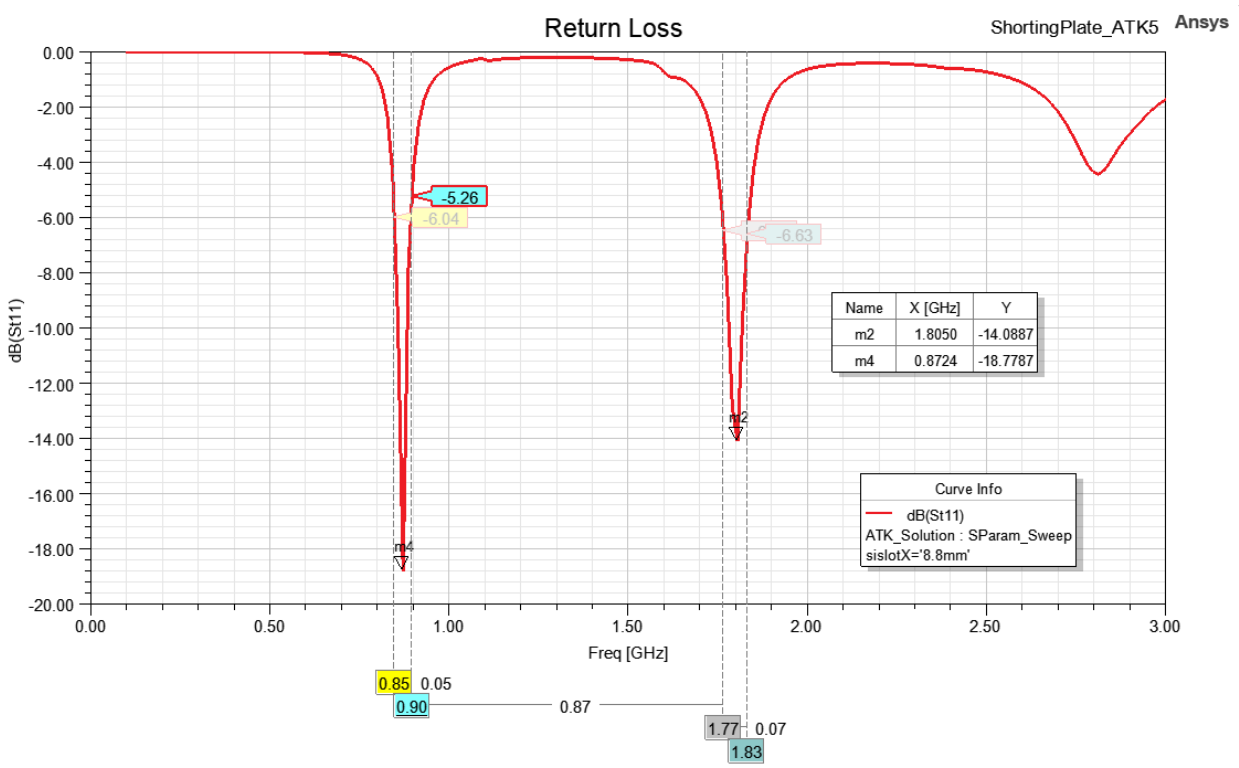

Figure 6. Return Loss for PIFA with Slot Structure

Quantity	Freq	Value	Freq	Value
Max U	0.872G...	99.105 mW/sr	1.8GHz	168.76 mW/sr
Peak Directivity		2.3398		3.7649
Peak Gain		1.2623		2.1935
Peak Realized...		1.2454		2.1207
Peak System ...		1.2454		2.1207
Radiated Power		532.27 mW		563.28 mW
Accepted Power		986.59 mW		966.79 mW

Figure 7. Antenna Parameters for two resonant mode of slotted PIFA

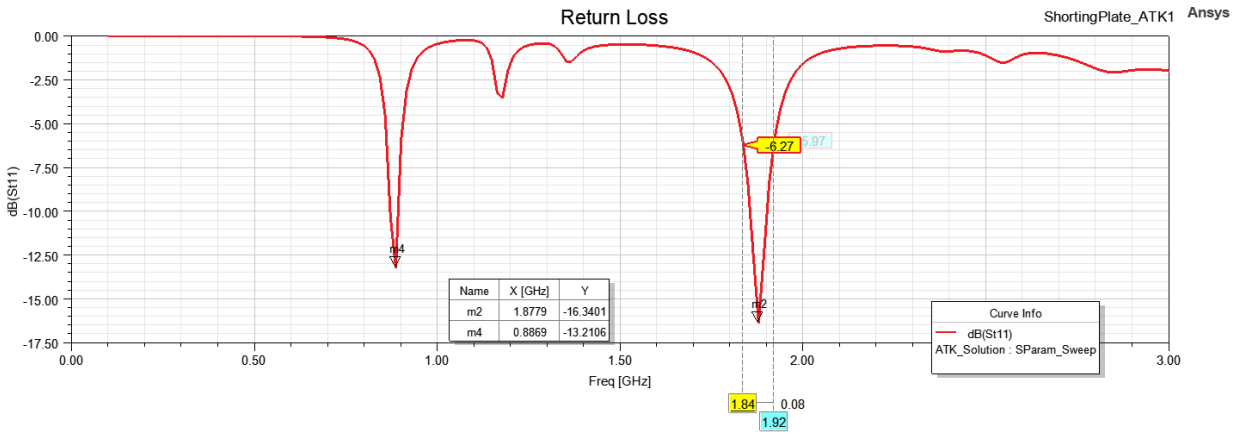

Figure 8. S11 plot for PIFA with parasitic element

Max U	0.887G...	80.008 mW/sr	1.88GHz	159.25 mW/sr
Peak Directivity		2.2874		3.2794
Peak Gain		1.0526		2.0494
Peak Realized...		1.0054		2.0013
Peak System ...		1.0054		2.0013
Radiated Power		439.55 mW		610.26 mW
Accepted Power		955.23 mW		976.52 mW

Figure 9. Radiation Efficiency of PIFA with parasitic element

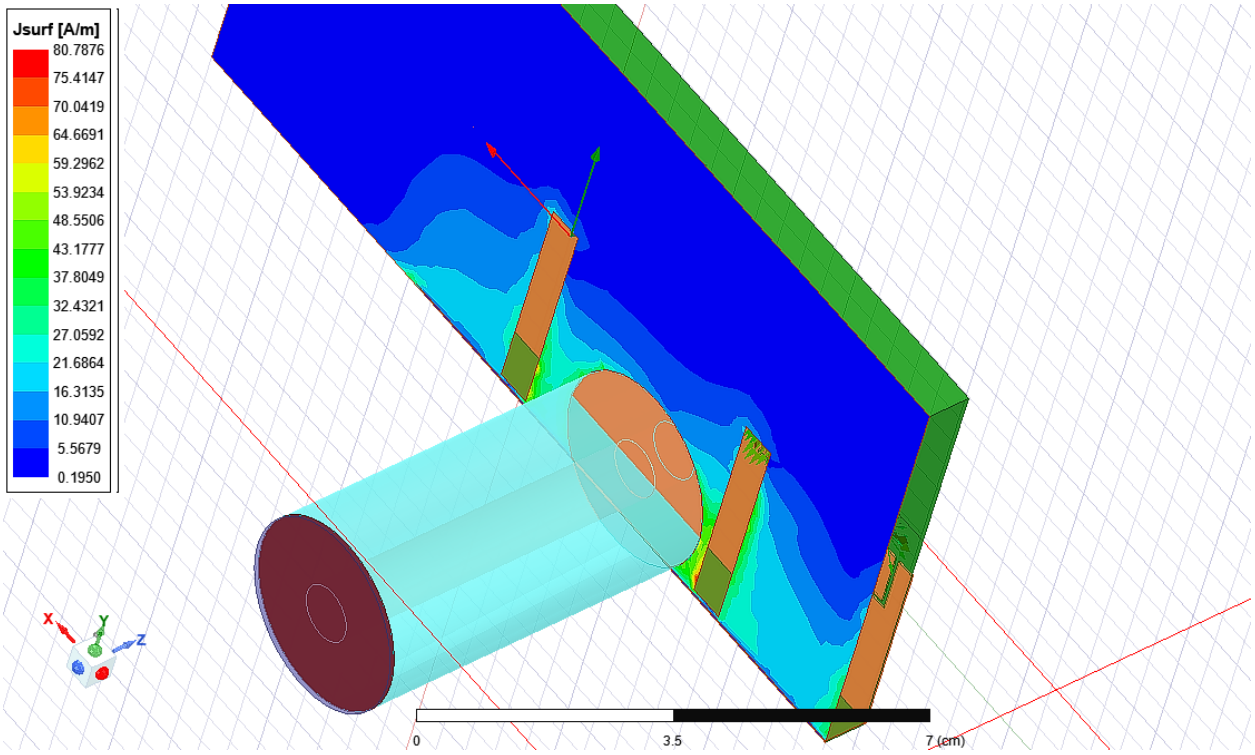

Figure 10. Slot added to Ground and the Current Distribution at lower the frequency.

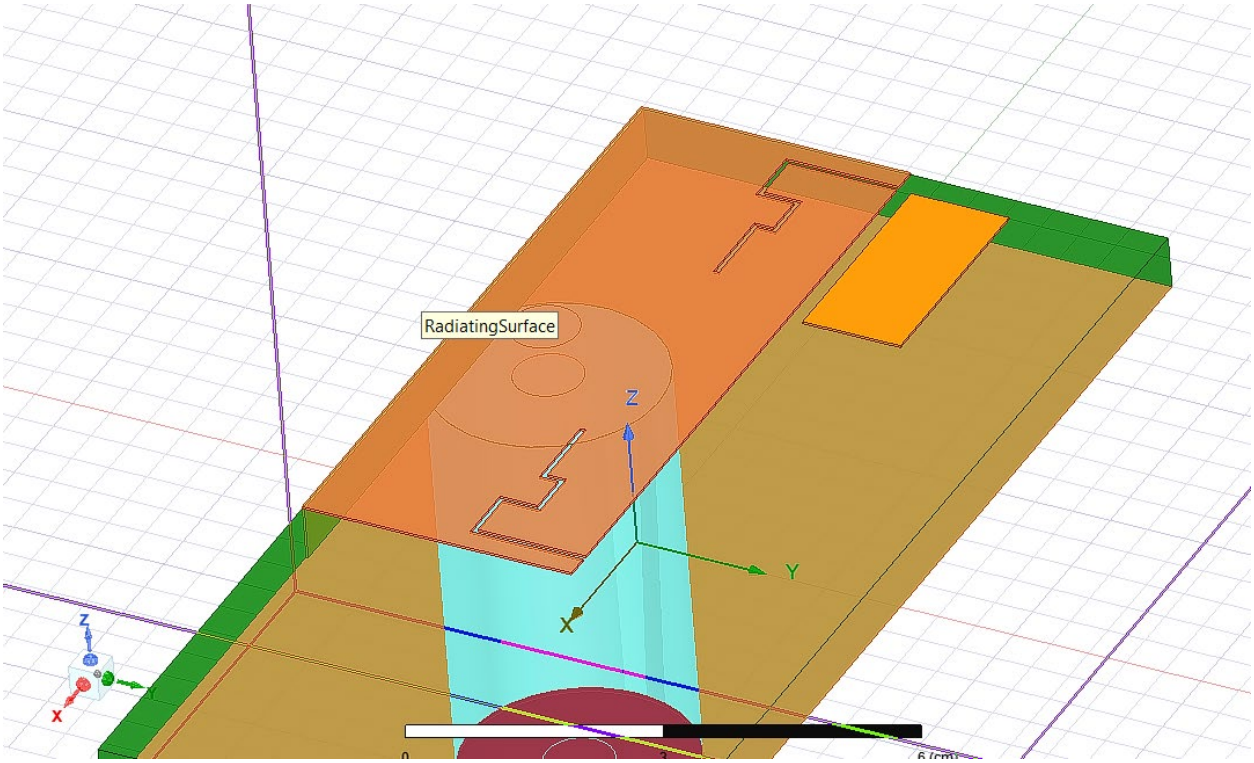

Figure 11. Second Slot added to PIFA.

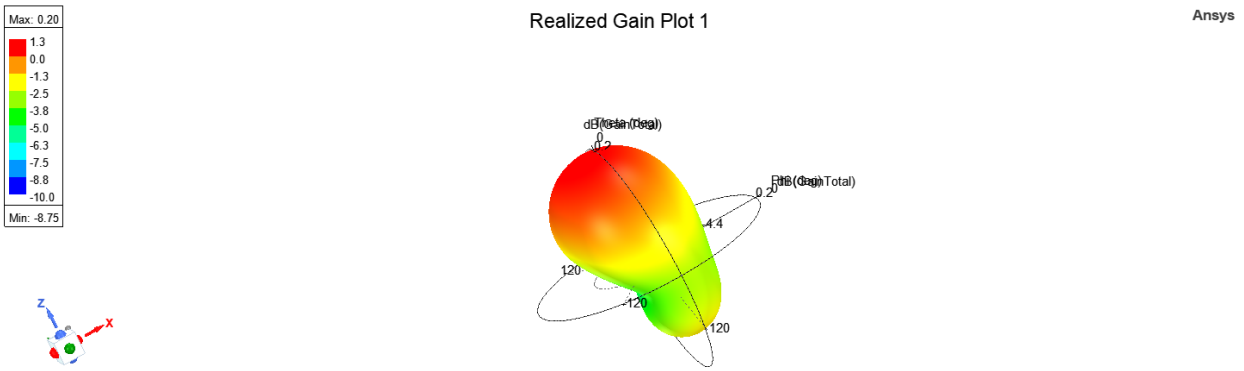

Figure 12. Radiation Pattern at Lower Frequency

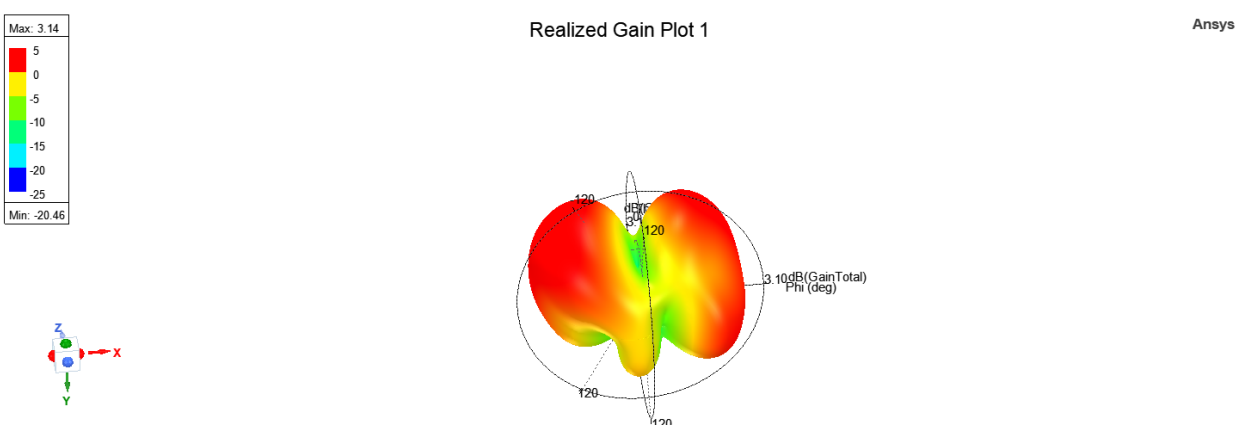

Figure 13. Radiation Pattern at Higher Frequency

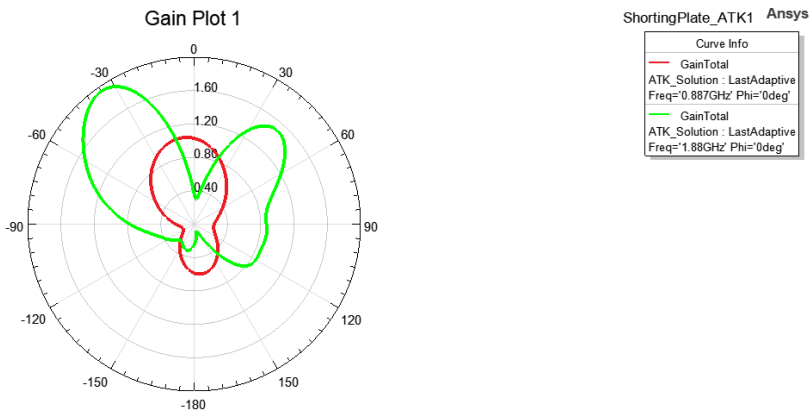

Figure 14. Elevation Plot for Phi = 0

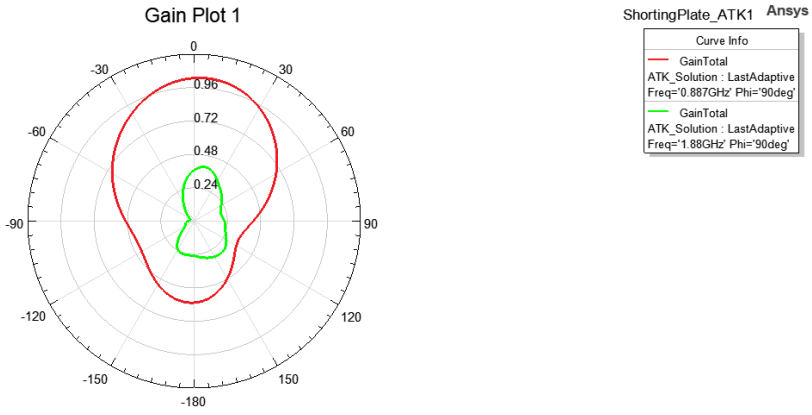

Figure 15. Elevation Plot for Phi = 90

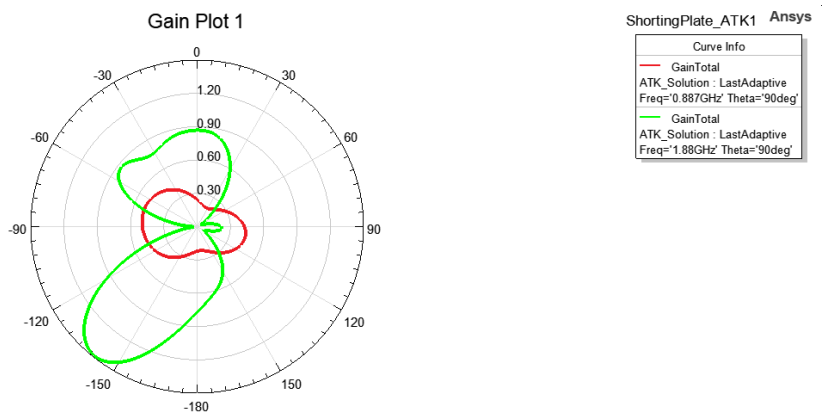

Figure 16. Azimuth Plot

Name	Freq [MHz]	Ang	Mag	RX
m1	886.93	107.8012	0.2157	0.8091 + 0.3486i
m2	1877.89	125.9744	0.1531	0.8116 + 0.2059i

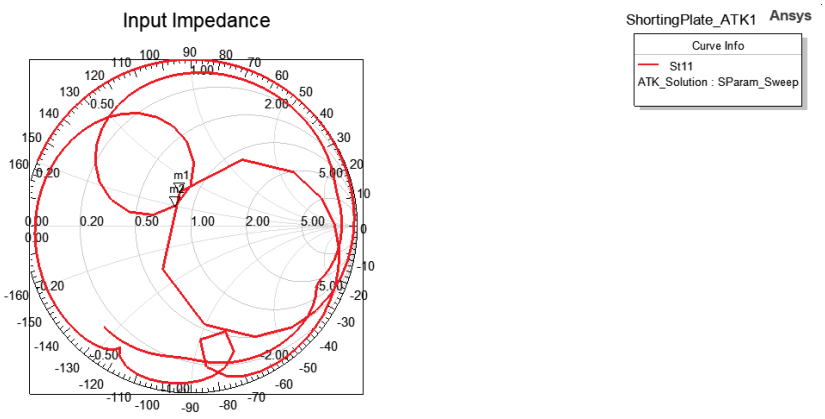

Figure 17. Input Impedance for the Resonant Frequency

Name	X [GHz]	Y
m1	0.8869	40.8894
m2	1.8779	41.0145

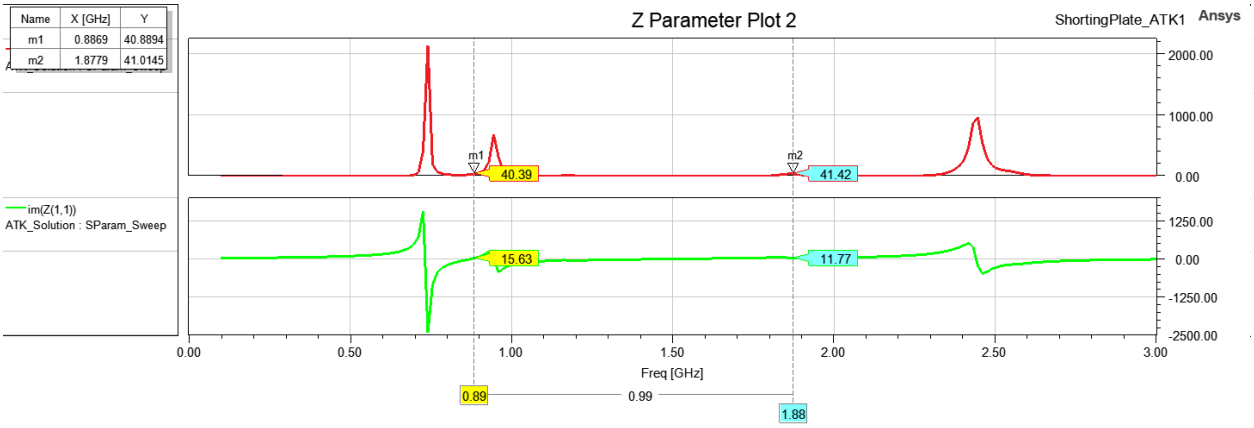

Figure 18. Real and Imaginary part for both resonant frequency

$$f = \frac{c}{4\sqrt{\varepsilon_r}(L + W - h - w_s)} \quad (1)$$

$$L = \frac{v_0}{2f_r}\sqrt{\frac{2}{\varepsilon_r + 1}} \quad (2)$$

$$\eta_r = \frac{P_r}{P_i} \quad (3)$$

References

[1] M. A. Fakih, A. Diallo, L. T. P. R. Staraj, O. Mourad and E. A. Rachid, "Optimization of Efficient Dual Band PIFA System for MIMO Half-Duplex 4G/LTE and Full-Duplex 5G Communications," *IEEE Access,* vol. 7, pp. 128881-128895, 2019, doi: 10.1109/ACCESS.2019.2940556.

[2] L. Luo, Hu, W. J. B, T. Yan and L.-J. Xu, "Compact dual-band antenna with slotted ground for implantable applications," *Microw Opt Technol Lett.,* vol. 61, p. 1314–1319. https://doi.org/10.1002/mop.31718, 2019.

[3] M. Agarwal and M. K. Meshram, "Bandwidth enhanced compact PIFA for dual band operation," in *2015 Radio and Antenna Days of the Indian Ocean (RADIO)*, Belle Mare, Mauritius, 2015.

[4] A. M. Lawan, H. T. Su, Y. L. Then and J. Zhang, "Parallel dual-slot PIFA for 2.45GHz rectenna applications," 2018 IEEE Sensors Applications Symposium (SAS)," in *Parallel dual-slot PIFA for 2.45GHz rectenna applications," 2018 IEEE Sensors Applications Symposium (SAS)*, Seoul, Korea (South), 2018.

[5] W. Ahmad and W. T. Khan, "Small form factor dual band (28/38 GHz) PIFA antenna for 5G applications," in *IEEE MTT-S International Conference on Microwaves for Intelligent Mobility (ICMIM)*, Nagoya, Japan, 2017.